PHYSICAL REVIEW B VOLUME 41, NUMBER 7 1 MARCH 1990

Neutron-diffraction study of the pressure-temperature phase diagram of $EuAs_3$

T. Chattopadhyay
Centre d'Etudes Nucléaires, Département de Recherche Fondamentale, Service de Physique, Groupe Magnétisme et Diffraction Neutronique 85X, 38041 Grenoble CEDEX, France and Institut Laue-Langevin, 156X, 38042 Grenoble CEDEX, France

P. J. Brown
Institut Laue-Langevin, 156X, 38042 Grenoble CEDEX, France
(Received 20 April 1989; revised manuscript received 10 October 1989)

Neutron-diffraction investigations have been performed on a single crystal of $EuAs_3$ under hydrostatic pressure up to 20 kbar. At pressures up to 2 kbar the magnetic structure is identical to that at ambient pressure. Above $P=2$ kbar, in addition to the collinear commensurate (AF1) and incommensurate (IC) phases, a helimagnetic phase (HP) develops below 2 K. At about $P=3$ kbar the commensurate phase is no longer stable and the sine-wave incommensurate phase transforms directly to the helimagnetic phase in which the magnetic moments are modulated in the (010) plane. At $P=18$ kbar the sine-wave phase itself becomes unstable and the helimagnetic phase develops directly from the paramagnetic phase. There are two triple points in the (P,T) phase diagram of $EuAs_3$: one at which the IC, AF1, and HP phases coexist and the other at which the paramagnetic, IC and HP phases coexist. This complicated behavior is quite unexpected for an S-state ion such as Eu^{2+}.

I. INTRODUCTION

There exist a number of magnetic systems[1] in which a sine-wave incommensurate magnetic phase develops at the ordering temperature. This sine-wave phase has a wave vector that is strongly temperature dependent. As the temperature is decreased the sine-wave phase undergoes a lock-in transition to a commensurate phase. A Landau description is appropriate, and if the moments are pinned along a crystal axis, e.g., the y axis, by an anisotropy, one is led to the soliton-lattice (SL) picture[2,3] described by an order parameter

$$S(\mathbf{r})=Ae^{i\phi(z)}e^{i\mathbf{q}_0\cdot\mathbf{r}}\ , \qquad (1)$$

where $A^2\sim T_N-T$, and $\phi(z)$ describes the modulation of the moment parallel to the y axis along the z direction; $\mathbf{q}_0$ is the commensurate lock-in wave vector. Immediately below the Néel temperature T_N, $\phi=\boldsymbol{\delta}\cdot\mathbf{r}$, where $\delta=\mathbf{q}_m-\mathbf{q}_0$ is parallel to $\hat{\mathbf{z}}$. At temperatures slightly above the lock-in temperature T_L, $\phi(z)$ is almost constant in a large region of z (commensurate region) separated by narrow regions (called phase solitons or domain walls), where $\phi(z)$ increases rapidly to reach the next commensurate value $n\cdot\pi/2$. The corresponding $\delta(T)$ is determined by the density of solitons as described by the sine-Gordon equation and is a smooth function of temperature. This behavior is found in many $4f$ and $5f$ systems with local moments and competing exchange interactions. Hydrostatic pressure often drastically modifies the magnetic properties of such a system. The situation can arise in which the paramagnetic, incommensurate, and the commensurate phases coexist at a triple point at higher pressure. If the modulation vector continuously approaches zero as this triple point is approached, then this triple point is a so-called Lifshitz point,[4] which has been extensively investigated theoretically. However, experimental realization of the Lifshitz point is rare in magnetic systems. The only known example is perhaps the triple point in the (H,T) phase diagram of MnP at which the paramagnetic, ferromagnetic, and fan phases coexist.[5] It would be more interesting to realize a Lifshitz point in the (P,T) phase diagram of a magnetic system because pressure is a simpler parameter than the magnetic field. Our recent investigations[6,7] on the magnetic properties of semimetallic $EuAs_3$ suggest that the occurrence of a Lifshitz point in the (P,T) phase diagram of this magnetic system is possible and our preliminary high-pressure neutron investigation suggested this also. In this paper we describe the results of our more detailed high-pressure neutron-diffraction investigations on $EuAs_3$. Although a true Lifshitz point is not realized in this system, the present neutron investigation has yielded interesting results. Apart from the above-mentioned commensurate (AF1) and incommensurate (IC) phases a third helimagnetic phase (HP) is stabilized at higher pressure leading to two triple points in the (P,T) phase diagram of $EuAs_3$, neither of which is a Lifshitz point.

$EuAs_3$ orders[6] at ambient pressure at $T_N=11$ K to an incommensurate sine-wave phase (Fig. 1) with a wave vector $\mathbf{k}=(-1,0,\frac{1}{2}-\delta)$. The modulation vector δ decreases continuously with decreasing temperature from $\delta=0.15$ at $T=11$ K, and at $T_L=10.3$ K this sine-wave phase undergoes a lock-in transition to a commensurate antiferromagnetic phase (AF1) with the wave vector $\mathbf{k}=(-1,0,\frac{1}{2})$. The magnetic moments of the Eu atoms are oriented parallel and antiparallel to the monoclinic b axis of the crystal. We have already shown that the temperature variation of the modulation vector follows the prediction of the sine-Gordon soliton-lattice theory despite some limitations of the application of this theory in this system.[6] The theory predicts a continuous lock-in transition, whereas actually we observe a sharp drop of δ at the lock-in transition as T_L is approached from the high-temperature side. The higher-order harmonics, predicted by the theory, close to the lock-in transition temperature have not been identified experimentally. We have reported[7] preliminary high-pressure investigations of the magnetic structure and phase diagram of $EuAs_3$. At $P=18$ kbar the commensurate and incommensurate phases are no longer stable and instead a helimagnetic phase (HP) develops directly from the paramagnetic phase at about $T=12$ K. The magnetic moments of the Eu atoms are modulated in the (010) plane (Fig. 1).

We have organized this paper in the following way: In Sec. II, we describe the experimental procedures. In Sec. III, we describe the crystal and magnetic structure of $EuAs_3$ at high pressure. In Sec. IV, we describe the neutron diffraction results leading to the pressure-temperature phase diagram of $EuAs_3$. In Sec. V, we describe the temperature induced sine-wave-to-commensurate transition at lower pressure and sine-wave-to-helimagnetic transition at higher pressure. In Sec. VI, we discuss the results on the basis of symmetry arguments and phenomenological Landau-type theory.

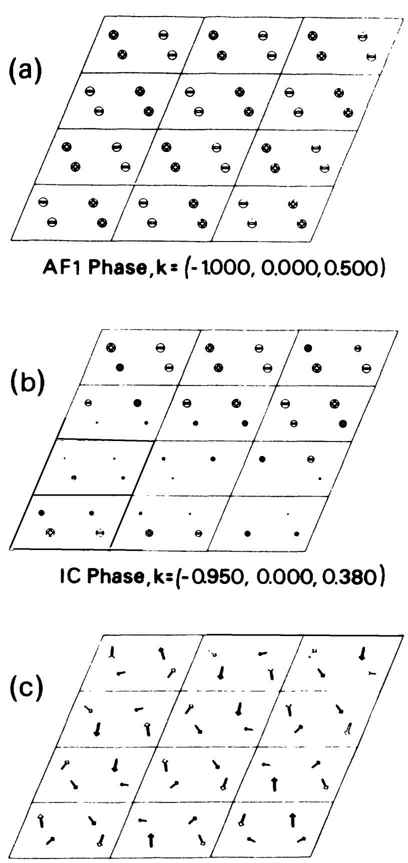

FIG. 1. Projection of the magnetic structures of (a) the antiferromagnetic phase AF1, (b) the incommensurate transverse sine-wave IC, and (c) the high-pressure helimagnetic phase HP of $EuAs_3$.

Finally in Sec. VII, we give the summary and main conclusions from the present investigations.

II. EXPERIMENTAL PROCEDURES

$EuAs_3$ was synthesized from the elements using Eu of 99.9% purity and As of 99.999% purity as starting materials. Large single crystals of dimensions of a few cm were grown by the Bridgman technique. The crystallographic orientations of the crystals were determined by back reflection x-ray Laue photographs. The crystals were then cut to a desired size by a diamond saw.

High-pressure neutron-diffraction experiments have been performed on $EuAs_3$ in the pressure range $0<P<20$ kbar. A He gas pressure cell was employed in the pressure range 0–4.6 kbar. High pressure was generated by a clamp system in the pressure range 5–20 kbar using deuterated methanol as the pressure medium. In the case of the He gas pressure cell the pressure was calibrated by measuring the resistance of a manganin gauge. For the clamp system the pressure was calibrated by measuring the lattice parameter of a NaCl crystal fixed at the side of the $EuAs_3$ crystal. Neutron-diffraction experiments were performed at the high-flux reactor of the Institut Laue-Langevin in Grenoble, with the diffractometer D15 in the normal beam geometry. The single crystal of $EuAs_3$ with size $1.5\times1.5\times5$ mm^3 was mounted in the pressure cell with its needle b axis parallel to the ω axis of the diffractometer.

III. CRYSTAL AND MAGNETIC STRUCTURE OF $EuAs_3$ AT HIGH PRESSURE

A. Crystal structure

$EuAs_3$ crystallizes with $BaAs_3$-type structure[8] (space group $C2/m$). The lattice parameters at room temperature and ambient pressure are $a=9.471(2)$ Å, $b=7.598(2)$ Å, $c=5.778(2)$ Å, $\beta=112.35(5)°$. The crystal structure consists of puckered As layers stacked along the [001] direction forming channels parallel to [010] in which Eu atoms are embedded. We have determined the lattice parameters at low temperatures and at different pressures in the range 0–20 kbar and these are given in Table I. The lattice parameters have been determined by centering about ten nuclear reflections at low temperatures. The lattice parameter b could not be determined because of the geometrical restrictions that did not allow us to center reflections hkl for $k>0$. Figure 2 shows the pressure variations of a, c, and β, which are found to be linear. The linear compressibilities in a and c are different as expected for the layered structure. The pressure variation of the lattice parameter shows the reliability of our pressure calibration. The crystal structure of $EuAs_3$ remains essentially unaltered in the pressure range 0–20 kbar. Substitution of As by P atoms reduces the volume of $EuAs_3$ and therefore generates chemical pressure. For comparison we give the lattice constants of $Eu(As_{1-x}P_x)_3$ at room and low temperatures in Table II. We note that the crystal structure of $Eu(As_{1-x}P_x)_3$ remains the same for $x\le0.98$. Pure EuP_3 exists in two

TABLE I. Pressure variation of the lattice parameters of $EuAs_3$.

P (kbar)	T (K)	a (Å)	b (Å)[a]	c (Å)	β (deg)	V (Å^3)	V/V_0
0	5.0	9.43(2)	7.50(1)	5.75(1)	112.48(5)	375.6	1.0
0.5	1.5	9.419(6)	7.49	5.749(4)	112.55(4)	374.6	0.9973
3	1.5	9.408(4)	7.46	5.731(3)	112.52(3)	374.1	0.9968
4.6	5.8	9.390(2)	7.42	5.718(1)	112.50(2)	368.1	0.9800
5	1.5	9.396(4)	7.41	5.723(3)	112.46(4)	366.8	0.9766
5	1.5	9.395(2)	7.41	5.721(2)	112.49(2)	368.0	0.9797
9	1.5	9.38(3)	7.26	5.71(2)	112.4(1)	359.5	0.9571
17	5.0	9.30(2)	7.19	5.66(8)	112.32(8)	350.1	0.9321
20	5.0	9.28(1)	7.14	5.642(9)	112.32(4)	345.8	0.9207

[a]b could not be determined because of geometrical restrictions. The given values are estimated values of b assuming the linear compressibility along the b axis is the average of those along the a and c axes.

modifications of which α-EuP_3 has the same crystal structure as that of $EuAs_3$, whereas β-EuP_3 has a modified crystal structure (SrP_3 type).[9]

B. Magnetic structure

We have determined the magnetic structure of $EuAs_3$ at $P=20$ kbar by using a clamp system. At this pressure the ambient pressure antiferromagnetic phase AF1 and the sine-wave IC phase no longer exist, instead a helimagnetic phase is stabilized at T_N. The wave vector was determined to be $\mathbf{k}=(-0.814,0,0.186)$ at $T=4$ K and $P=20$ kbar. The details of the magnetic structure analysis of the high-pressure (HP) phase of $EuAs_3$ are given in the Ref. 7. The HP phase of $EuAs_3$ is a helimagnetic phase in which the magnetic moments lie in the (010) plane and are modulated both in direction and amplitude describing the envelope of an ellipse. The components of the magnetic moment along the major and minor axes of the ellipse are $S_x=7.2(4)\mu_B$ and $S_y=4.4(4)\mu_B$, respectively. The angle α between S_x and a^* axis is refined to be $\alpha=117(3)°$. The major axis S_x of the ellipse, therefore makes an angle of 27° from the crystallographic c axis in the acute β. The results are given in Table III and have been compared with the low-temperature helimagnetic phase[10,11] of $Eu(As_{0.02}P_{0.98})_3$ and the field-induced SF1 phase of $EuAs_3$.[25] In Fig. 1 we show the projection of the helimagnetic high-pressure phase (HP) of $EuAs_3$. The wave vector is approximately antiparallel to the crystallographic a axis and makes an angle of about 45° to the major and minor axes of the ellipse of the moments. There is apparently no simple way to understand the orientation of this ellipse. The wave vector, the orientation of the ellipse, and its axial ratio of the helimagnetic phases of $EuAs_3$ and $Eu(As_{i-x}P_x)_3$ are highly sensitive to the temperature, pressure, and magnetic field. This is probably due to the sensitivity of the "competition ratio" of the exchange interactions of $EuAs_3$ (see Sec. VI A) on these external parameters.

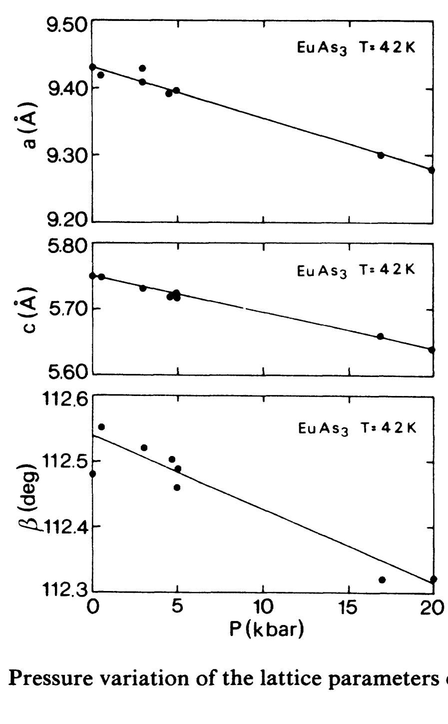

FIG. 2. Pressure variation of the lattice parameters of $EuAs_3$.

IV. PRESSURE-TEMPERATURE PHASE DIAGRAM

We have already reported[7] high-pressure neutron-diffraction experiments leading to the pressure-temperature diagram of $EuAs_3$ up to $P=4.6$ kbar. At pressures up to $P=2$ kbar, the magnetic structure of $EuAs_3$ is identical to that at ambient pressure. Above $P=2$ kbar, in addition to the collinear commensurate (AF1) and incommensurate (IC) phases, a helimagnetic phase (HP) develops below 2 K. For 3 kbar $\leq P \leq 4.6$ kbar the commensurate phase is no longer stable and the sine-wave incommensurate phase transforms directly to the helimagnetic phase. We have additionally performed similar experiments at $P=5$ and 9 kbar with a clamp system. At $P=5$ kbar, the situation is similar to that ob-

TABLE II. Lattice parameters of $Eu(As_{1-x}P_x)_3$ (Ref. 11).

x	T (K)	a (Å)	b (Å)[a]	c (Å)	β (deg)	V (Å^3)	V/V_0
0	5.0	9.43(2)	7.50(1)	5.75(1)	112.48(5)	375.6	1.0
0.10	15.0	9.370(7)	7.46	5.722(5)	112.53(3)	369.4	0.9835
0.40	25.0	9.257(5)	7.35	5.675(3)	112.78(4)	356.0	0.9478
0.80	2.0	9.08(2)	7.20	5.59(1)	112.95(6)	336.5	0.8959
0.98	4.2	9.059(5)	7.13	5.576(1)	113.15(3)	331.2	0.8818

[a] b could not be determined because of geometrical restrictions. The given values are estimated values of b assuming the concentration dependence of b at low temperatures is the same as that at room temperature (Refs. 8 and 9).

tained at $P=4.6$ kbar. $EuAs_3$ orders at $T_N=10.9$ K to the IC phase, which transforms to the HP phase at 9.9 K. At $P=9$ kbar the IC phase could no longer be found and the HP phase directly develops from the paramagnetic phase at $T_N=10.33$ K. Similar results were obtained previously[7] at $P=18$ and 20 kbar. A second-order phase transition from the paramagnetic phase to a helimagnetic phase is inconsistent[7] with the monoclinic symmetry of $EuAs_3$. However, the massive high-pressure cell used in these experiments did not allow us to determine the character of the helimagnetic phase transition at T_N with certainty; neither have we determined the magnetic structure of the HP phase close to T_N. Therefore the controversy raised in Ref. 7 still remains unsettled.

Figure 3 shows the (T,P) phase diagram of $EuAs_3$. The phase diagram shows a triple point at $T=9.8$ K and $P=2.9$ kbar, where the incommensurate, commensurate, and the helimagnetic phases coexist. There is another triple point in the phase diagram where the incommensurate sine-wave, the high-pressure helimagnetic phase, and the paramagnetic phases coexist. We have not been able to localize it in the phase diagram. This triple point should exist at $T=10$ K with P between 5 and 9 kbar. Figure 1 illustrates the three different magnetic structures. Figure 4 also shows the (T,x) diagram of $Eu(As_{1-x}P_x)_3$ taken from Ref. 10. One should note a close similarity in this (T,P) diagram and the (T,x) diagram of $Eu(As_{1-x}P_x)_3$. The pressure parameter seems to be analogous to the concentration x. However, because single crystals were not available at enough concentrations, we could not determine the value of x for which the commensurate phase transforms into the helimagnetic phase. For $x=0.80$ and 0.98 we have determined the structure of the helimagnetic phase and have found this to be identical to that of the high-pressure phase found in the present investigations. The similarity of the (P,T) phase diagram of $EuAs_3$ and the (T,x) phase diagram of $Eu(As_{1-x}P_x)_3$ can be qualitatively understood. Substitution of the As atom by the smaller P atom is somewhat equivalent to the application of pressure.

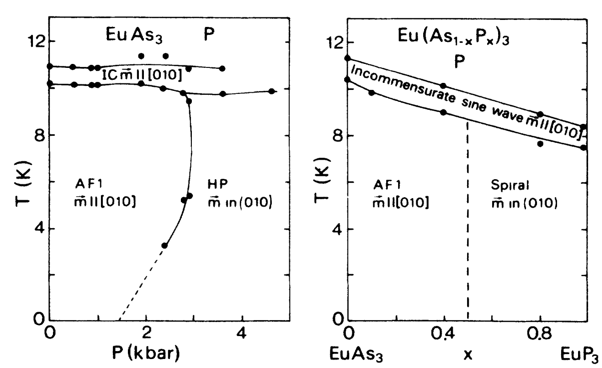

FIG. 3. The magnetic (T,P) phase diagram of $EuAs_3$ has been compared with the (T,x) phase diagram of $Eu(As_{1-x}P_x)_3$. There exists a triple point at $P=2.9$ kbar and $T=9.8$ K in the (T,P) phase diagram of $EuAs_3$ at which AF1, HP, and IC phases coexist. The phase diagram also suggests that a further triple point might exist at P between 5 and 9 kbar and $T=10$ K at which IC, HP, and the paramagnetic (P) phase coexist. The similarities between the (T,P) phase diagram of $EuAs_3$ and the (T,x) phase diagram of $Eu(As_{1-x}P_x)_3$ are evident.

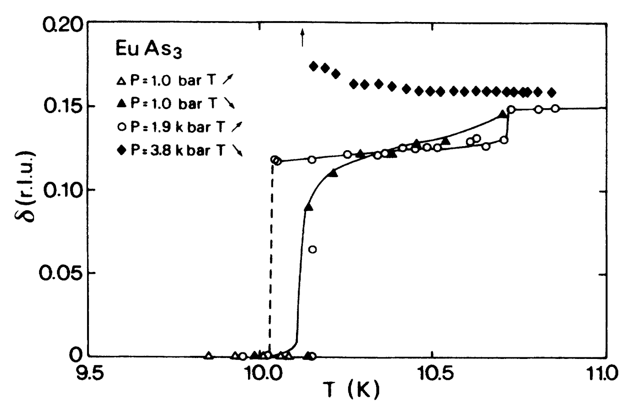

FIG. 4. Temperature variation of the modulation vector δ of the sine-wave IC phase at different pressures.

V. TEMPERATURE DEPENDENCE OF THE WAVE VECTOR

A. Sine-wave–to–commensurate transition

Figure 4 shows the temperature variation of the modulation vector δ of the sine-wave phase at $P=1$ bar, 1.9 and 3.8 kbar. At ambient pressure we have already shown that the temperature dependence of the wave vector follows the prediction of the sine-Gordon soliton-lattice model. At pressures $P<1.9$ kbar similar behavior is observed. At $P=1.9$ kbar the temperature variation of the modulation vector is found to be linear and is practically constant. At $T=10.7$ K the modulation vector decreases discontinuously with decreasing temperature from $\delta=0.15$ to 0.13, at $T_L=10.05$ it drops discontinuously to zero. There is a hysteresis of about 0.1 K at the lock-in transition, indicating the first-order nature of the transition. Similar behavior has been observed by substituting As atoms by P atoms in $EuAs_3$. At $P=3.8$ kbar the modulation vector δ increases with decreasing temperature. At this pressure the incommensurate sine-wave phase does not lock into the commensurate phase, instead it undergoes a sine-wave to helimagnetic phase transition—the wave vector therefore does not approach $(\bar{1},0,\frac{1}{2})$; it approaches the wave vector of the helimagnetic phase, which is $\mathbf{k}=(-0.89,0,0.22)$.

Figure 5 shows the intensities obtained in q scans parallel to c^* through the reciprocal point $(-1,0,\frac{1}{2})$ as a function of temperature at 1 bar and 1.9 kbar. At 1 bar a pair of satellites starts to develop at 10.17 K that increases very rapidly in intensity and moves away from the commensurate position $(-1,0,\frac{1}{2})$ as the temperature rises above T_L. The satellite intensity decreases again at higher temperature and can no longer be observed above 10.9 K, but the separation of the satellites increases continuously with temperature until they disappear. The component of the wave vector parallel to $\mathbf{c}^*$ is found to vary smoothly from an extrapolated value of 0.35 at T_N to the commensurate value $\frac{1}{2}$ at T_L. The value of the wave vector was determined in heating and cooling cycles and no significant hysteresis was observed. No second- or higher-order satellites were observed. A second-order satellite, if it exists, has less than 5% of the intensity of the first-order satellite at 10.4 K. At $P=1.9$ kbar the scenario of the lock-in transition looks different. At $T=10.02$ K only the commensurate reflection at $(-1,0,\frac{1}{2})$ is observed. At $T=10.15$ K the $-1,0,\frac{1}{2}$ reflection is still observed along with five satellites at $l=0.375$, 0.435, 0.565, 0.580, and 0.610. The temperature was not quite stable and varied from 10.12 to 10.18 K during the scan. It is very difficult to understand the presence of these five satellites. The peak at $l=0.58$ does not fit to any scheme. This is definitely of magnetic origin as is shown by its disappearance at higher temperature. The temperature instability or gradient might have led to its origin. The remaining four peaks can be grouped with two modulation vectors, $\delta_1=\pm0.065$ and $\delta_2\simeq2\delta_1\simeq0.120$. It is not quite certain whether δ_2 could be considered as the second-order harmonic of δ_1. The

TABLE III. The magnetic structure of the high-pressure phase of $EuAs_3$ at $P=20$ kbar and a comparison with the low-temperature spiral phase ICPI of $Eu(As_{0.02}P_{0.98})_3$ and the field-induced phase SF1 of $EuAs_3$. α = angle between the a^* axis and the major axis S_x of the ellipse, S_x,S_y = components of the magnetic moments along the major and the minor axes of the ellipse, respectively, N = number of independent reflections, and R = agreement factor between the observed and calculated structure factors.

Compound	Phase	T (K)	P (kbar)	H (T)	Wave vector	α (deg)	S_x (μ_B)	S_y (μ_B)	N	R	Reference
$EuAs_3$	HP	4.0	20	0	$(-0.814,0,0.186)$	117(3)	7.2(3)	4.4(4)	32	0.15	This work
$Eu(As_{0.02}P_{0.98})_3$	ICP1	4.0	0	0	$(-0.726,0,0.222)$	99(2)	7.3(2)	4.5(1)	209	0.15	11
$EuAs_3$	SF1	4.0	0	1.25	$(-0.9,0,0.25)$	90	5.3	4.6	42	0.15	25

peaks corresponding to δ_2 have a higher intensity than the intensities of the peaks corresponding to δ_1. As the temperature is raised the satellites $\delta_1 = \pm 0.065$ disappear and those at $\delta_2 = \pm 0.12$ move away from each other. However, as we have shown in Fig. 4 the temperature variation of δ no longer follows a smooth-lattice behavior but is linear. At $T = 10.66$ K two pairs of peaks are observed corresponding to two wave vectors $\delta_1 = 0.13$ and 0.16, of which those corresponding to δ_1 have larger intensity. At $T = 10.72$ K the peaks corresponding to δ_2 have a higher intensity than those corresponding to δ_1. At $T = 10.80$ peaks corresponding to δ_1 have disappeared and only those corresponding to δ_2 are seen. Similar phenomenon has already been observed[6] at ambient pressure before. We have investigated this only on heating and therefore the possible hysteresis effects are not known.

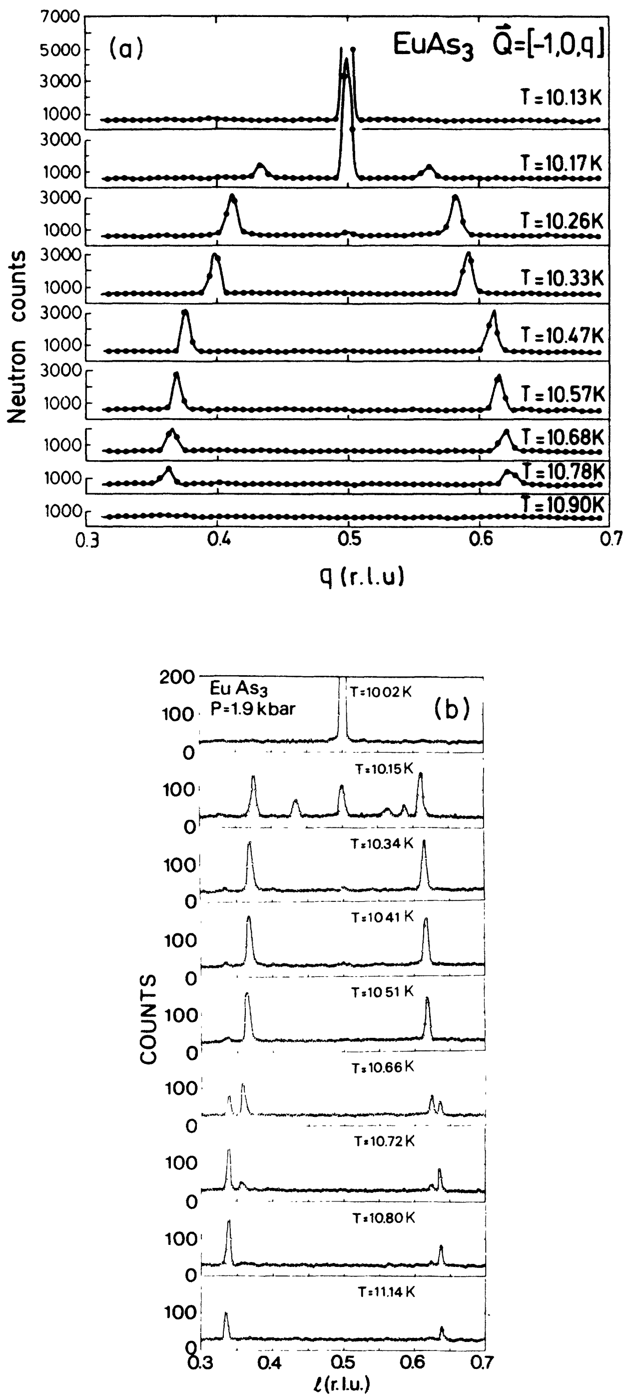

FIG. 5. Temperature variation of the intensity obtained in q scans parallel to c^* through $(-1,0,\frac{1}{2})$ at $P = 1$ kbar and $P = 1.9$ bar.

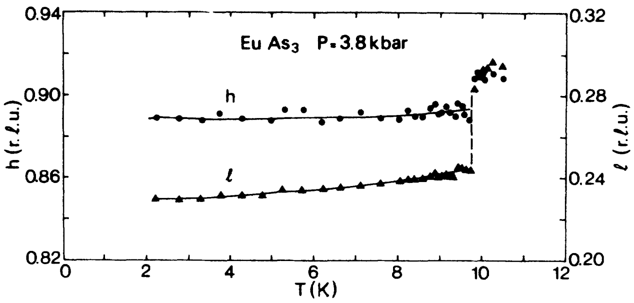

FIG. 6. Temperature variation of the components h and l of the wave vector parallel to $\mathbf{a}^*$ and $\mathbf{c}^*$, respectively, at $P = 3.8$ kbar. At $T = 9.75$ K discontinuities corresponding to a first-order transition from a sine-wave (IC) to a helimagnetic phase (HP) are observed. This sine-wave-to-helimagnetic phase transition has already been observed in phosphorus-rich $Eu(As_{1-x}P_x)_3$ at ambient pressure (Ref. 10).

B. Sine-wave–to–helimagnetic transition

Figure 6 shows the temperature variation of the components of the wave vector h and l parallel to $\mathbf{a}^*$ and $\mathbf{c}^*$, respectively, on heating at $P = 3.8$ kbar. In the helimagnetic phase h and l increase with increasing temperature. At about 9.8 K both components increase discontinuously, indicating a first-order helimagnetic–to–sine-wave transition. We have reported a similar phase transition[10] in $Eu(As_{1-x}P_x)_3$ for $x = 0.80$ and 0.98.

VI. DISCUSSION

The magnetic pressure-temperature diagram of $EuAs_3$ is rather complex considering that the Eu^{2+} ion is in the $^8S_{7/2}$ ground state with zero orbital moment. The origin of this complex behavior is not yet understood. One can speculate that the proximity of the Eu $4f$ level to the Fermi level in this semimetallic system might lead to hybridization of the $4f$ states with the conduction electron states—a situation that might be quite analogous to that found in CeSb.[13] Since the electronic band structure of $EuAs_3$ is not known, it is difficult to conclude anything beyond this intuitive speculation. In the absence of the microscopic theory, phenomenological Landau type theory and symmetry arguments are quite useful to understand the complex behavior of $EuAs_3$.

A. Exchange model

Thalmeier[14] has performed a simple model calculation to gain some insight into the origin of the modulated structure of $EuAs_3$. This calculation is based on anisotropic Heisenberg exchange

$$H_{ex} = -\frac{1}{2}\sum_{\substack{ll' \\ \alpha\alpha'}} I_{ll'}^{\alpha\alpha'} S_l^{\alpha} S_{l'}^{\alpha'} \ , \tag{2}$$

where the suffix l,l' refers to the unit cell and α,α refers to the basis atoms. The Eu neighbors of any Eu^{2+} ion can be separated into a nearest-neighbor (NN) group (distance ~3.01–4.29 Å) and a next-nearest-neighbor (NNN) group (distance ~5.76–5.99 Å). From inspection of the commensurate antiferromagnetic phase (AF1) the exchange interaction constants $I_0, I_1 > 0$ for the NN exchange and $I_2 < 0$ for the NNN exchange. Note that neighboring $(\bar{2}01)$ planes are coupled both ferromagnetically (I_0) and antiferromagnetically (I_2), whereas the coupling to the second-nearest-neighbor planes is neglected since Eu distances become rather large (> 8 Å) for them. Since (at ambient pressure) the moments are oriented along $\pm\mathbf{b}$ for all temperatures below T_N, a sufficiently strong anisotropy potential $\sim D[S_y^2 - \frac{1}{3}(S+1)]$ must also exist which is, however, not included explicitly. With this simple exchange model, by varying the competition ratio $r = -I_2/I_1 > 0$ and the anisotropy ratio $r' = I_0/I_1 > 0$ Thalmeier[14] has generated the phase diagram in (r,r') parameter plane shown in Fig. 7. AF1 and AF2 are different antiferromagnetic commensurate phases. FM is the ferromagnetic phase and IC is the incommensurate phase. For an isotropic NN exchange ($r'=1$) only a ferromagnetic and AF1 phase can exist but no modulated phase. The situation

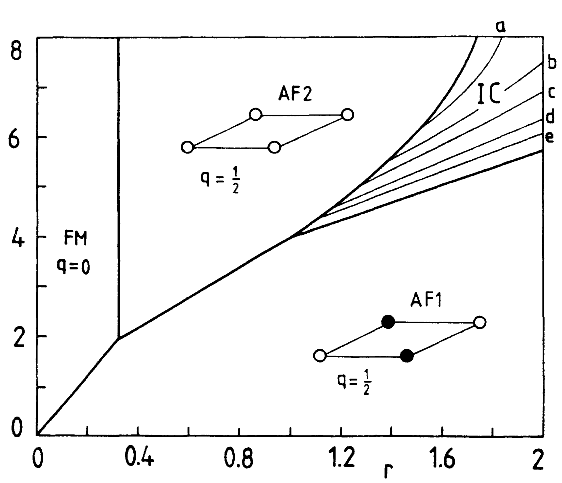

FIG. 7. Phase diagram of $EuAs_3$ for $T \le T_N$ in the (r,r') parameter plane (Ref. 14). AF1 and AF2 are antiferromagnetic phases, FM is the ferromagnetic and IC is the incommensurate phase. The IC region is shown with contours for $\delta(r,r') = \frac{1}{2} - q_m$. curves (a)–(e): δ=0.14, 0.13, 0.12, 0.11, and 0.10, respectively.

for $(r,r') = (1.6, 5.7)$ is quite close to the experimental observations in $EuAs_3$ at ambient pressure for which an incommensurate phase is stabilized at T_N. At lower temperature this incommensurate phase undergoes a lock-in transition to the commensurate AF1 phase. The magnetic moments are parallel to $\pm\mathbf{b}$ in both the phases. Since the hydrostatic pressure does not modify r and r' in the same way it is expected to modify drastically the stabilities of the phases of $EuAs_3$. As we have shown in previous sections this is indeed so. At lower pressures $P < 2$ kbar the situation is qualitatively the same as that at ambient pressure. In the pressure range 2 kbar $< P < 3$ kbar in addition to the IC and AF1 phases a helimagnetic high-pressure phase is stabilized at a lower temperature in which the magnetic moments are modulated in the (010) plane. At $P \ge 3$ kbar the IC phase transforms directly to the HP phase and the AF1 phase is no longer stabilized. The transformation from the IC phase to the helimagnetic high-pressure HP phase involves spin reorientation from the [010] direction to the (010) plane. Thalmeier[14] has not calculated the stability of the helimagnetic phase.

B. Similarities between the effects of hydrostatic pressure and phosphorus substitution

As we have already noted in Sec. V the temperature-pressure diagram of $EuAs_3$ is remarkably similar to the temperature-concentration phase diagram of the system $Eu(As_{1-x}P_x)_3$. Figure 3 shows these two diagrams together. The phase boundary between the AF1 phase and the helimagnetic phase in $Eu(As_{1-x}P_x)_3$, which has not been located exactly, has been tentatively shown as a dotted vertical line at $x = 0.5$. In reality this phase boundary could be curved as in the temperature-pressure phase diagram of $EuAs_3$. It is, however, not surprising that the effect of hydrostatic pressure is somewhat equivalent to that of P substitution. P atoms having smaller atomic radii than those of As, substitution of As by P is expected to generate chemical pressure. However, considering that full substitution of As by P causes a volume change of about 12%, a volume change of 6% (Vegard's law is well obeyed by this system) occurs at $x = 0.5$ for which the AF1 to HP transition takes place. This volume change is much larger than the volume change caused by 3 kbar (about 0.5%) at which the AF1-HP transition takes place in $EuAs_3$. Therefore, the volume effect cannot be the principal driving mechanism of the AF1→HP phase transition in $EuAs_3$. The detailed electronic structure must be highly sensitive to hydrostatic pressure. If the p-f hybridization effect is responsible for the complex magnetic behavior of $EuAs_3$ and $Eu(As_{1-x}P_x)_3$ one can well imagine this to be highly pressure sensitive. This has been also found in CeSb (Ref. 15), where of course the crystal-field effects cause additional complexities. In the system $Eu(As_{1-x}P_x)_3$ galvanomagnetic measurements[12] show that the charge carrier density decreases drastically by the substitution of As atoms by P atoms. The charge carrier density of $EuAs_3$ at 3 K is 9.8×10^{20} cm^{-3}. For $Eu(As_{1-x}P_x)_3$ the charge carrier density at 3 K is 2.2×10^{19} cm^{-3} and 2.3×10^{18} cm^{-3} for $x = 0.40$ and

0.98, respectively. The charge carrier density in $EuAs_3$ is likely to decrease on application of hydrostatic pressure. So far no galvanomagnetic measurements of $EuAs_3$ under hydrostatic pressure have been performed to check this.

C. Sine-wave–to–commensurate transition

The pressure-temperature phase diagram of $EuAs_3$ is unique in the way that it provides the opportunity to investigate several types of novel phase transitions. At ambient pressure and also at pressures up to 2 kbar a transverse sine-wave modulation develops at T_N that undergoes a lock-in transition to the commensurate phase. The commensurate structure is characterized by the wave vector $\mathbf{K}$ belonging to some symmetry point of the Brillouin zone, whereas the incommensurate structure is characterized by the wave vector $\mathbf{K}+\mathbf{k}$, where $\mathbf{k}$ is usually very small. As the temperature is lowered the wave vector of the incommensurate structure often changes either continuously or discontinuously, and at some temperature T_L locks into the commensurate value $\mathbf{K}$. Landau-type continuum theory can be applied to this lock-in transition, provided $\mathbf{k}$ is small and the stability range of the incommensurate phase $T_N - T_L$ is relatively small, i.e., $|T_N - T_L| \ll T_N$. Two distinct types of continuum theory for the incommensurate phase exist.[16] In the first type the thermodynamic potential taken as function of the order parameter contains a Lifshitz invariant, whereas in the second it does not. Type-I continuum theory leads to the well-known soliton-lattice description in which the incommensurate phase is truly sinusoidal close to T_N, but just above T_L it consists of relatively large regions of commensurate phase separated by narrow regions of discommensuration, domain walls, or phase solitons.[2,3] In this theory the wave vector of the incommensurate phase varies smoothly with temperature and the lock-in transition is of the second order; higher-order satellite reflections should in principle appear just above T_L. In type-II theory[17,18] the structure of the incommensurate phase continues to be practically sinusoidal down to the lock-in transition, which is distinctly of the first order. At ambient pressure the incommensurate sine-wave phase of $EuAs_3$ can be described by the type-I theory.[6] The temperature dependence of the wave vector follows the sine-Gordon soliton-lattice behavior. However, the higher-order satellites predicted by the type-I theory close to T_L have not been experimentally observed. We have shown[19] that for $Eu(As_{1-x}P_x)_3$ the temperature variation of the wave vector crosses over from the soliton-lattice behavior of the $EuAs_3$ to a linear behavior for $x = 0.40$. The effect of hydrostatic pressure is very similar and at about P = 1.9 kbar the similar crossover to the linear behavior is observed. It is to be noted that the above-mentioned crossover takes place at approximately the same pressure or P substitution where the HP phase begins to appear. The temperature variation of the wave vector in the IC phase is also linear (Fig. 4) at pressures for which the IC phase transforms into the HP phase. The phase transition at T_L is prominently of the first order. This result is more in consistence with the type-II continuous theory. However, at P = 1.9 kbar we have observed higher-order satellite reflections close to the lock-in transition that have not been observed at the ambient pressure. The reverse situation would be expected if the system crosses over from the type-I to the type-II situation. The present experimental observations suggest that the two extreme descriptions of the lock-in transitions can only be partially true and the actual situation is more complicated. Since the microscopic theory of the lock-in transition does not exist, it is difficult to understand how hydrostatic pressure or P substitution could lead to a completely different lock-in transition.

D. Antiferromagnetic-to-helimagnetic phase transition

In the pressure range 2 kbar $< P < 3$ kbar we have shown that $EuAs_3$ orders with a sine-wave phase that undergoes a lock-in transition at T_L to the antiferromagnetic AF1 phase. However, at lower temperature the antiferromagnetic phase undergoes a further phase transition to a helimagnetic phase. This phase transition from the higher temperature antiferromagnetic phase to the low temperature incommensurate phase is rather unusual. This type of phase transition has been observed in $NiBr_2$.[20–22] This behavior is typical of the system that is very close to a Lifshitz point. It is well-known that for a certain value of the exchange coupling constants, Heisenberg or XY magnets can have, at $T=0$ a helimagnetic structure,

$$\langle \mathbf{S}_i \rangle = S(\mathbf{u}\cos\mathbf{Q}\cdot\mathbf{R}_i + \mathbf{v}\sin\mathbf{O}\cdot\mathbf{R}_i) , \tag{3}$$

where $\mathbf{u}$, $\mathbf{v}$ are orthogonal unit vectors, S_i is the spin at site R_i, and $\mathbf{O}$ is the wave vector. Villain[23] has shown that, when the helical ordering is the stable state at $T=0$, with increasing temperature, magnetic excitations induce fluctuations between the helical states of opposite chirality, which drives the system to a commensurate phase. Although Villain[23] has considered the helimagnetic-to-ferromagnetic transition, a recent Monte Carlo simulation[24] shows similar results for the helimagnetic-to-antiferromagnetic transition. In $EuAs_3$ at the helimagnetic-to-antiferromagnetic transition the magnetic moments reorient from the (010) plane to the [010] direction and the above-mentioned theories and calculations need appropriate modifications–although Villain's general conclusions may be still valid.

E. Sine-wave-to-helimagnetic transition

At $P \geq 3$ kbar the antiferromagnetic AF1 phase is no longer stable in $EuAs_3$ and the sine-wave incommensurate phase transforms directly to the helimagnetic phase. According to the group theory[1] for orthorhombic or lower symmetry, the irreducible representations are only one dimensional and therefore, in theory, helimagnetic ordering cannot develop with a second-order phase transition. This is in accordance with the observation for $EuAs_3$ and $Eu(As_{1-x}P_x)_3$ for which the phase transition at T_N is of the second order. With purely isotropic exchange interactions and a single-ion anisotropy of easy-plane type the energies of the two order parameters can be accidentally degenerate and a linear combinations of these order parameters can lead to a helical structure that has the same energy as the sine-wave modulation. In this case the phase transition should be either of the first order or rather complex, with two successive phase transitions. Let us consider in the case of an easy plane with the wave vector in this plane, the dipolar energy makes the energy of the component perpendicular to the wave vector $\mathbf{k}$ ($\mathbf{m}_{\mathbf{k}}^{\perp}$) more favorable than that of the parallel component $\mathbf{m}_{\mathbf{k}}^{\parallel}$. The system prefers to adopt a sine-wave modulation at T_N. As the temperature is lowered, a phase transition to a helimagnetic structure is expected because the helimagnetic structure has lower energy at lower temperatures. The transition can be very close to T_N when isotropic exchange interactions dominate anisotropic ones. This situation seems to be fulfilled for $EuAs_3$ and $Eu(As_{1-x}P_x)_3$. We have in fact observed the sine-wave-to-helimagnetic transition[10,11] in $Eu(As_{1-x}P_x)_3$ for $x=0.80$ and 0.98. We also observed the same type of transition in $EuAs_3$ at pressure ≥ 3 kbar. In the helimagnetic phases found in $EuAs_3$ under pressure and in $Eu(As_{1-x}P_x)_3$ the moment value is distributed on an ellipse instead of a circle as for a classical structure. This is also what is expected in $EuAs_3$ because there is no reason to assume that the two Eu atoms of the Bravais sublattices have the same moment value when they have different orientations. To our knowledge this sine-wave–to–helical phase transition observed in $EuAs_3$ under pressure or with the substitution of the P atoms is the first example of such a phenomena to be observed in any magnetic system. It is not yet understood why this transition is favored for high P-atom concentration and also at higher pressure. Probably this is related with the change of detailed electronic structure under pressure and/or with P substitution.

VII. SUMMARY AND CONCLUSIONS

We have determined the pressure-temperature phase diagram of $EuAs_3$ by neutron diffraction up to 20 kbar. At pressures up to 2 kbar the magnetic structure is identical to that at ambient pressure. A transverse sine-wave phase is developed at T_N with a wave vector that is strongly temperature dependent. The magnetic moments are parallel to the b axis. As the temperature is lowered this incommensurate phase undergoes a lock-in transition at T_L to an antiferromagnetic phase. The temperature variation of the modulation vector in the incommensurate phase follows the prediction of the sine-Gordon soliton-lattice theory. At $P=1.9$ kbar temperature variation of the modulation vector no longer follows the sine-Gordon theory but crosses over to a linear behavior. Above $P=2$ kbar, in addition to the collinear antiferromagnetic (AF1) and incommensurate (IC) phases, a helimagnetic phase (HP) phase develops below 2 K. At about $P=3$ kbar the commensurate phase is no longer stable and the sine-wave phase transforms directly to the helimagnetic phase in which the magnetic moments are modulated in the (010) plane. At $P=9$ kbar the sine-wave phase itself becomes unstable and the helimagnetic phase develops directly from the paramagnetic phase. There are two triple points in the (P,T) phase diagram of $EuAs_3$: one at which the IC, AF1, and HP phases coexist and the other at which the paramagnetic P, IC, and HP phases coexist. We have localized the first triple point in the (P,T) phase diagram, whereas the second triple point needs further investigations.

From the basis of the present investigations the following conclusions are made:

(1) The semimetallic $EuAs_3$ has rather complex magnetic properties considering that Eu^{2+} ion is in $^8S_{7/2}$ ground state with no orbital moment. However, by assuming anisotropic exchange interaction the stabilities of the commensurate and incommensurate phases of $EuAs_3$ can be phenomenologically understood.

(2) The temperature variation of the modulation vector of the incommensurate IC phase of $EuAs_3$ follows the prediction of the sine-Gordon soliton-lattice theory at the ambient pressure. However, the higher-order satellite reflections that would in principle appear close to T_L have not been experimentally observed at the ambient pressure.

(3) At about $P=2$ kbar the temperature variation of the modulation vector of the IC phase no longer follows the sine-Gordon functional but crosses over to a linear behavior. The lock-in transition is dominantly of the first order. Curiously enough, we observe second-order satellite reflections at this pressure close to T_L, whereas according to the theory they should have been observed at ambient pressure rather than at higher pressure. This suggests that lock-in transition has not yet been understood theoretically in details and the two extreme models described in Sec. VI do not represent the actual situation.

(4) The microscopic reason for the crossover from a soliton-lattice behavior to the linear behavior is not understood but must be related to the change of the detailed electronic structure with pressure.

(5) (P,T) phase diagram of $EuAs_3$ enables one to study three kinds of the novel phase transitions: (a) sine-wave–to–commensurate lock-in transition, (b) an antiferromagnetic-to-helimagnetic transition, and (c) sine-wave–to–helimagnetic transition. It is possible that the system is very close to the Lifshitz point. The Lifshitz point may be reached by the substitution of As with Sb, which would generate negative chemical pressure.

(6) The temperature phase diagram of $EuAs_3$ is remarkably similar to the temperature-concentration phase diagram of $Eu(As_{1-x}P_x)_3$. We have shown in Sec. VI that this is not due to the volume effect alone but has to be attributed to the similarity in the change of electronic structure because of hydrostatic pressure and P substitution.

(7) As a final conclusion we add that the semimetallic $EuAs_3$ and the solid solutions $Eu(As_{1-x}P_x)_3$ show magnetic behavior that is as exciting as those of CeSb.[13] The origin of anisotropy is not understood at the present state of knowledge. However, the proximity of the Eu $4f$ state to the Fermi level in the semimetallic $EuAs_3$ might lead the p-f hybridization to give rise to anisotropy.

ACKNOWLEDGMENTS

We wish to thank Professor H. G. von Schnering for his encouragement and support. The present investigations have been performed at the high flux reactor of the Institut Laue-Langevin, and we wish to acknowledge instrumental facilities of this Institute. We wish to thank Mr. G. Melesi and Mr. P. Andant for their technical help and Dr. C. Vettier for his help and advice in the high-pressure techniques.

[1]J. Rossat-Mignod, in *Neutron Scattering in Condensed Matter,* edited by K. Skold and D. L. Price (Academic, New York, 1986).

[2]P. Bak and J. v. Boehm, Phys. Rev. B **21**, 5297 (1980).

[3]W. L. McMillan, Phys. Rev. B **14** 1496 (1976).

[4]R. M. Hornreich, M. Luban, and S. Shtikman, Phys. Rev. Lett. **35**, 1678 (1975).

[5]Y. Shapira, in *Proceedings of the NATO Advanced Study Institute of Multicritical Phenomena, Geilo, Norway, 1983,* edited by R. Pynn and A. Skjeltrop (Plenum, New York), p. 53.

[6]T. Chattopadhyay, P. J. Brown, P. Thalmeier, and H. G. v. Schnering, Phys. Rev. Lett. **57**, 372 (1986).

[7]T. Chattopadhyay and P. J. Brown, Phys. Rev. B **36**, 2454 (1987); T. Chattopadhyay and P. J. Brown, Physica B **156&157**, 737 (1989).

[8]W. Bauhofer, M. Wittmann, and H. G. von Schnering, J. Phys. Chem. Solids **42**, 687 (1984).

[9]M. Wittmann, W. Schmettow, D. Semmer, W. Bauhofer, and H. G. von Schnering, in Proceedings of the Sixth International Conference of Transition Elements, Stuttgart, 1979 (unpublished).

[10]T. Chattopadhyay and P. J. Brown, Phys. Rev. B **36**, 7300 (1987).

[11]T. Chattopadhyay, P. J. Brown, P. Thalmeier, W. Bauhofer, and H. G. von Schnering, Phys. Rev. B **37**, 269 (1988).

[12]W. Bauhofer, E. Gmelin, M. Mollendorf, R. Nesper, and H. G. von Schnering, J. Phys. C **18**, 3017 (1985).

[13]J. Rossat-Mignod, J. M. Effantin, P. Burlet, T. Chattopadhyay, L. P. Regnault, H. Bartholin, C. Vettier, O. Vogt, D. Ravot, and J. C. Achart, J. Magn. Magn. Mater. **52**, 111 (1985).

[14]P. Thalmeier, J. Magn. Magn. Mater. **58**, 207 (1986).

[15]T. Chattopadhyay, P. Burlet, J. Rossat-Mignod, H. Bartholin, C. Vettier, and O. Vogt, J. Magn. Magn. Mater. **63&64**, 52 (1987).

[16]A. P. Levanyuk, in *Incommensurate Phases in Dielectrics-I: Fundamentals,* edited by R. Blink and A. P. Levanyuk (North-Holland, Amsterdam, 1986), p. 1.

[17]A. Michelson, Phys. Rev. B **16**, 577 (1977).

[18]A. D. Bruce, R. A. Cowley, and A. F. Murray, J. Phys. C **11**, 3591 (1978).

[19]T. Chattopadhyay, P. J. Brown, and H. G. von Schnering, Europhys. Lett. **6**, 89 (1988).

[20]P. Day, A. Dinsdale, E. R. Krausz, and D. J. Robbins, J. Phys. C **9**, 2481 (1976).

[21]K. Katsumata and M. Date, J. Phys. Soc. Jpn. **27**, 1360 (1969).

[22]Y. Morito and M. Date, J. Phys. Soc. Jpn. **29**, 1090 (1970).

[23]J. Villain, Physica **86-88B**, 631 (1977).

[24]J. Villain (private communication).

[25]W. Bauhofer, U. Steigenberger, and P. J. Brown, J. Magn. Magn. Mater. **67**, 49 (1987).